Kinetics of the Daunomycin–DNA Interaction†

Jonathan B. Chaires,*,‡ Nanibhushan Dattagupta,§ and Donald M. Crothers§

Department of Biochemistry, The University of Mississippi Medical Center, Jackson, Mississippi 392116-4505, and Department of Chemistry, Yale University, New Haven, Connecticut 06511
Received July 9, 1984

ABSTRACT: The kinetics of the interaction of daunomycin with calf thymus DNA are described. Stopped-flow and temperature-jump relaxation methods, using absorption detection, were used to study the binding reaction. Three relaxation times were observed, all of which are concentration dependent, although the two slower relaxations approach constant values at high reactant concentrations. Relaxation times over a wide range of concentrations were gathered, and the data were fit by a minimal mechanism in which a rapid bimolecular association step is followed by two sequential isomerization steps. The six rate constants for this mechanism were extracted from our data by relaxation analysis. The values determined for the six rate constants may be combined to calculate an overall equilibrium constant that is in excellent agreement with that obtained by independent equilibrium measurements. Additional stopped-flow experiments, using first sodium dodecyl sulfate to dissociate bound drug and second pseudo-first-order conditions to study the fast bimolecular step, provide independent verification of three of the six rate constants. The temperature dependence of four of the six rate constants was measured, allowing estimates of the activation energy of some of the steps to be made. We speculate that the three steps in the proposed mechanism may correspond to a rapid "outside" binding of daunomycin to DNA, followed by intercalation of the drug, followed by either conformational adjustment of the drug or DNA binding site or redistribution of bound drug to preferred sites.

The anthracycline antibiotics daunomycin and adriamycin are widely used in cancer chemotherapy. The effects of these drugs on the cell are pleiotropic and may involve interaction of the drugs with receptors on the cell membrane, with proteins, and with nucleic acids (Gianni et al., 1982). This latter interaction may be of particular importance, since daunomycin and adriamycin are potent inhibitors of both DNA replication and RNA synthesis (Ward et al., 1965; Hartmann et al., 1964; DiMarco et al., 1971; Goodman et al., 1977; Schellinx et al., 1979; Barthelemy-Clavey, 1976) and indications are that the inhibition requires a direct interaction of the drugs with DNA.

Accordingly, numerous studies have focused on the details of the daunomycin–DNA interaction [Graves & Krugh, 1983; for extensive reviews of earlier literature, see Arcamone (1981) and Gianni et al. (1982)]. Work from our laboratories has examined equilibrium aspects of the daunomycin–DNA interaction (Chaires et al., 1982; Chaires, 1983a, 1984), the geometry of the daunomycin–DNA complex (Fritzsche et al., 1982), the binding of the drug to nucleosomes (Chaires et al., 1983), the sequence specificity of the daunomycin–DNA interaction (Chaires, 1983a), and the effects of the drug on the B $\rightleftharpoons$ Z transition in poly(dG-dC) (Chaires, 1983b). A complete understanding of the daunomycin–DNA interaction requires, in addition to such equilibrium information, knowledge of the kinetics of the binding reaction. Kinetic studies provide information necessary for the formulation of a plausible reaction mechanism, which is essential for understanding the binding process in molecular detail. In addition, the biological and pharmacological activity of drugs may often be more readily correlated with kinetic rather than equilibrium properties of the drug–DNA complex (Mueller & Crothers, 1968; Crothers, 1971). Finally, kinetic information is required to completely understand the influence of drugs on molecular transformations of nucleic acids, such as the B $\rightleftharpoons$ Z transition (Mirau & Kearns, 1983).

The kinetics of the interaction of daunomycin with DNA are described here. Our primary goal is to establish a plausible reaction mechanism for the binding of daunomycin to DNA. Changes in the absorbance of daunomycin at 480 nm that occur with binding were used to monitor the binding process in stopped-flow and temperature-jump relaxation kinetic experiments. A minimal mechanism in which the drug binds to DNA in a rapid bimolecular step, followed by two sequential isomerizations, is consistent with our experimental data. The six rate constants for this mechanism extracted from our data may be used to calculate an overall equilibrium constant that is in excellent agreement with the binding constant obtained from independent equilibrium measurements. More conventional stopped-flow experiments monitoring dissociation steps by the sodium dodecyl sulfate (SDS) dissociation method (Mueller & Crothers, 1968), and the bimolecular step by mixing experiments under pseudo-first-order conditions, provide independent verification of three of the six rate constants. While the molecular events corresponding to each kinetic step are at this point unknown, we speculate that the three steps may correspond to the rapid formation of an "outside" complex, followed by drug intercalation, followed by either conformational adjustments of the drug–DNA complex or redistribution of bound drug to preferred sites by internal transfer.

Materials and Methods

DNA Preparation. High molecular weight calf thymus DNA was purchased from Boehringer-Mannheim (Indianapolis, IN) and sonicated, digested with RNase and proteinase K, phenol extracted, and fractionated as previously described (Chaires et al., 1982b). DNA samples were dialyzed exten-

† Supported by Grant 5 S07 RR05386 awarded by the Biomedical Research Support Grant Program, National Institutes of Health, and by U.S. Public Health Service Grants CA 35635 (to J.B.C.) and CA 15583 (to D.M.C.) awarded by the National Cancer Institute, Department of Health and Human Services.
‡ The University of Mississippi Medical Center.
§ Yale University.

0006-2960/85/0424-0260$01.50/0

sively against BPES buffer [6 mM Na_2HPO_4, 2 mM NaH_2PO_4, 1 mM disodium ethylenediaminetetraacetate (Na_2EDTA), and 0.185 M NaCl, pH 7.0] prior to binding or kinetic experiments. An extinction coefficient of 12 824 M^{-1} (bp) was used to calculate DNA concentrations from absorbance measurements at 260 nm.

Equilibrium Binding Studies. Spectrophotometric titration was used to determine the binding isotherm for the daunomycin–DNA interaction as previously described (Chaires et al., 1982b; Chaires, 1983). Drug was added to a DNA solution in BPES, and the absorbance at the isosbestic point, 540 nm, and at 480 nm was recorded following each addition. The concentration of total drug was calculated from

$$C_T = A_{540}/5100\ M^{-1}\ cm^{-1}$$

and the concentration of bound drug estimated from

$$C_b = (C_T\epsilon_{480} - A_{480}^{obsd})/\Delta\epsilon$$

where ϵ_{480} = 11 500 M^{-1} cm^{-1}, A_{480}^{obsd} is the measured absorbance at 480 nm, and $\Delta\epsilon$ has been previously determined to be 4500 M^{-1} cm^{-1} (Chaires et al., 1982b). The concentration of free drug was then obtained by difference:

$$C_f = C_T - C_b$$

Binding data were cast into the form of a Scatchard plot (Scatchard, 1949) and fit to the neighbor-exclusion model (McGhee & von Hippel, 1974; Crothers, 1968):

$$r/C_f = K(1 - nr)\{(1 - nr)/[1 - (n - 1)r]\}^{n-1} \quad (1)$$

where r is the ratio of bound drug to total DNA base pairs, K is the binding constant to an isolated site, and n is the exclusion parameter. Fitting was performed with a nonlinear least-squares fitting routine available on the NIH PROPHET computer resource.

Stopped-Flow Studies. Stopped-flow studies were made on a Dionex D-110 stopped-flow spectrophotometer using absorption detection at 480 nm, a 1:1 mixing ratio, and a 20-mm path-length cuvette. The dead time of the instrument is less than 2 ms, as judged by the reaction of $Fe(NO_3)_3$ in H_2SO_4 with NaCNS. Data were recorded photographically from a Tektronix 5111A storage oscilloscope. Photographs were digitized by using a Tektronix 4953 graphics tablet and analyzed as described below.

Mixing experiments were initiated by mixing DNA solution in BPES buffer with an equal volume of dialysate buffer containing daunomycin. The concentration of potential DNA binding sites was maintained in excess of the perturbation of site concentration resulting from drug binding. This allows for the data to be treated by the methods of relaxation kinetics (Hiromi, 1979). For each mixing experiment, reactants were mixed in a 1:1 ratio manually, allowed to equilibrate, and analyzed spectrophotometrically as described above to determine the final concentration of free and bound drug, and unoccupied DNA sites.

Digitized photographic traces were analyzed individually by least-squares fits of semilog plots of ln $(A_\infty - A_t)$ vs. time where A_∞ is the infinite time base line. Alternatively, individual traces were combined to form a composite time course of the binding process, as a plot of $A_\infty - A_t$ vs. time. Typically, 12 traces, each covering a discrete time range, were combined to produce the composite time course. The data were then fit to multiple exponentials by using a least-squares fitting routine based on the Marquardt–Levenberg algorithm available through the NIH PROPHET computer resource. Initial estimates were generated by a "peeling" process in which the tail of a semilog plot of the time course was fit by a line which was then subtracted from the remaining points. Remaining points were then treated by the same procedure until estimates for the desired number of exponentials had been obtained. These initial guesses provided the starting values for the least-squares fitting routine. The analysis of individual traces and the composite time course yielded similar results, although the latter approach was used primarily since the method provided more statistically reliable and consistent results.

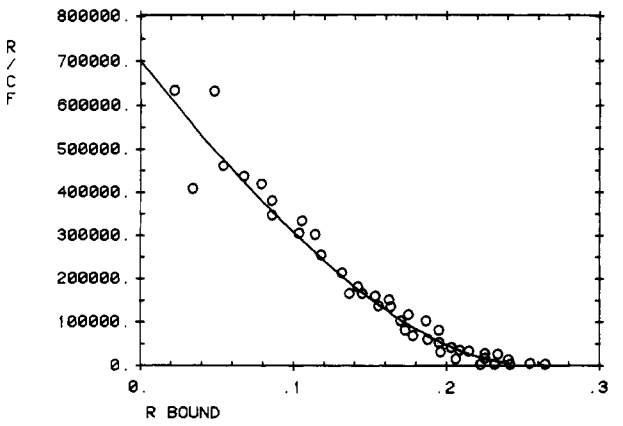

FIGURE 1: Binding isotherm for the daunomycin–calf thymus DNA interaction. Solution conditions were 6 mM Na_2HPO_4, 2 mM NaH_2PO_4, 1 mM Na_2EDTA, and 0.185 M NaCl, pH 7.0, 20 °C. The distribution of free and bound drug was determined spectrophotometrically as described in the text. The line is the nonlinear least-squares fit of the experimental data to the neighbor-exclusion model (eq 1) for $n = 3.6 \pm 0.1$ bp and $K = (7.0 \pm 0.25) \times 10^5\ M^{-1}$.

Dissociation rates were measured by the SDS method of Mueller & Crothers (1968). Preformed daunomycin–DNA complexes were mixed with an equal volume of SDS in BPES buffer to give a final detergent concentration of 1% (w/v). Data were recorded, digitized, and analyzed as described above.

Temperature-Jump Relaxation Kinetics. The temperature-jump apparatus and the overall methodology used in these studies have been described (Crothers, 1971; Bresloff & Crothers, 1975).

Solutions for temperature-jump experiments were prepared by equilibrium dialysis. A DNA solution in BPES at high concentration [0.5–1.0 mM (bp)] was dialyzed against a daunomycin–BPES solution until equilibrium was reached. The free and bound drug concentrations were then determined spectrophotometrically (Chaires et al., 1982b). A series of solutions of varying DNA concentration were then prepared by dilution of the concentrated complex with the dialysate, ensuring a constant value of r (the amount of drug bound per base pair) over the concentration range used.

Data were recorded photographically and relaxation times obtained from a semilog plot of amplitude vs. time using 15–20 points from each photograph. In some cases, kinetic curves were fed directly into a PDP-11 computer, via a Biomation Model 805 transient recorder, and relaxation times were obtained by least-squares regression. The results were indistinguishable from the manual analysis results.

RESULTS

Equilibrium Results. Figure 1 shows the binding isotherm, as a Scatchard plot, for the daunomycin–DNA interaction. For data above $r_b = 0.05$, the data are best fit by the neighbor-exclusion model, yielding $K = 7.0 \times 10^5\ M^{-1}$ and $n = 3.6$ base pairs (bp).

Stopped-Flow Relaxation Studies. Figure 2 shows examples of the primary data obtained from stopped-flow mixing

Table I: Analysis of the Stopped-Flow Data of Figure 3[a]

fit	multiple R^2	SD (V)	$1/\tau_1$ (s)	$1/\tau_2$ (s)	$1/\tau_3$ (s)
one exponential	0.9700	0.0618	44.7 ± 1.0		
two exponentials	0.9957	0.0233	148.5 ± 4.0	13.9 ± 0.5	
three exponentials	0.9966	0.0207	226.9 ± 15.0	46.2 ± 5.2	4.0 ± 1.0

[a] Data were fit to single or multiple exponentials as described in the text. The total optical signal was 1.0 V.

Table II: Summary of Estimated Rate Constants[a]

k_{12} (M^{-1} s^{-1})	k_{21} (s^{-1})	K_{12} (M^{-1})	k_{23} (s^{-1})	k_{32} (s^{-1})	K_{23}	k_{34} (s^{-1})	k_{43} (s^{-1})	K_{34}	comments
$3.0\ (\pm 0.4) \times 10^6$	168 ± 21	1.8×10^4	92.5 ± 13	11.2 ± 5.5	8.3	4.2 ± 0.5	1.0 ± 0.5	4.0	stopped-flow, relaxation analysis, 21 °C
2.8×10^6				5.5 ± 1.2			1.2 ± 0.2		stopped-flow, conventional analysis, 21 °C
$7.0\ (\pm 1.2) \times 10^6$	342 ± 29	2.0×10^4							T jump, 33 °C

[a] Rate constants were obtained from the experimental data of Figures 4–6 by assuming the mechanism of Scheme I. Solution conditions in all cases were 6 mM Na_2HPO_4, 2 mM NaH_2PO_4, 1 mM Na_2EDTA, and 0.185 M NaCl, pH 7.0.

Scheme I

$$\mathrm{DM} + \mathrm{DNA} \underset{k_{21}}{\overset{k_{12}}{\rightleftharpoons}} \mathrm{DM{-}DNA} \underset{k_{32}}{\overset{k_{23}}{\rightleftharpoons}} (\mathrm{DM{-}DNA})^{*} \underset{k_{43}}{\overset{k_{34}}{\rightleftharpoons}} (\mathrm{DM{-}DNA})^{**}$$

experiments. Such data were used to construct a composite time course for the binding process, an example of which is shown in Figure 3A. A semilog plot of this time course is nonlinear (not shown), indicating that multiple exponentials are required to describe the binding kinetics. Three exponentials are, in fact, necessary to fit the time course, as judged by two criteria. First, residual plots for fits of the experimental data to one and two exponentials show nonrandom deviations, whereas the residuals for the three-exponential fit appear randomly distributed (Figure 3B–D). Second, the statistics of the fit steadily improve up to the inclusion of three exponentials (Table I). Addition of a fourth exponential results in no improvement of the fit and nonsensical negative values for the fourth rate constant and was therefore unwarranted.

The concentration dependence of the three relaxation times was studied over a wide range of DNA and drug concentrations, with the results shown in Figure 4. The fastest observed reciprocal relaxation time increases linearly over the concentration range studied, while the two slower reciprocal relaxation times increase at low concentrations but tend toward constant values at high concentrations.

A minimal mechanism to account for these observations is shown in Scheme I where daunomycin (DM) interacts with DNA in a rapid bimolecular step, which is followed by two sequential isomerizations. This mechanism predicts three relaxation times, defined by

$$1/\tau_1 = k_{12}[\text{DNA sites} + \text{free drug}] + k_{21} \quad (2)$$

$$1/\tau_2 = k_{23}\left(\frac{[\text{DNA sites} + \text{free drug}]}{K_{21} + [\text{DNA sites} + \text{free drug}]}\right) + k_{32} \quad (3)$$

$$1/\tau_3 = k_{34}\left\{\frac{K_{12}K_{23}[\text{DNA sites} + \text{free drug}]}{1 + K_{12}[\text{DNA sites} + \text{free drug}](1 + K_{23})}\right\} + k_{43} \quad (4)$$

where $K_{12} = 1/K_{21} = k_{12}/k_{21}$, $K_{23} = k_{23}/k_{32}$, and the rapid equilibration of the preceding step has been assumed in each case.

Because of the site-exclusion effects shown by daunomycin (Chaires et al., 1982b; Figure 1), the concentration terms in eq 2–4 must be specified as described by Jovin & Stricker (1977):

$$[\text{DNA sites} + \text{free drug}] = f(r)C_0 - f'(r)C_f$$

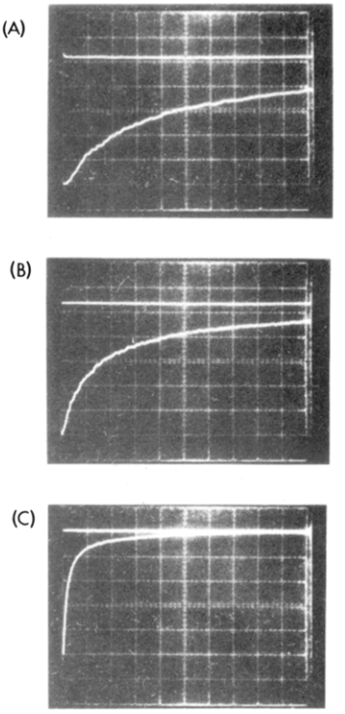

FIGURE 2: Samples of primary data from stopped-flow mixing experiments. DNA in BPES was mixed with an equal volume of daunomycin dissolved in dialysate solution to yield a final DNA concentration of 79.5 μM (bp) and a final daunomycin concentration of 10 μM at 21 °C. The association of drug was monitored by changes in transmittance at 480 nm. For all the oscilloscope traces, the ordinate scale is 0.2 V per division. The abscissa scale is (A) 2 ms per division, (B) 5 ms per division, or (C) 50 ms per division.

where C_0 is the total concentration of DNA binding sites, C_f is the concentration of free drug, and

$$f(r) = \frac{(1 - nr)^n}{[1 - (n - 1)r]^{n-1}}$$

$$f'(r) = \frac{[nr(n - 1) - 2n + 1](1 - nr)^{n-1}}{[1 - (n - 1)r]^n}$$

where r is the ratio of bound drug to the total number of DNA binding sites and n is the exclusion parameter.

The data of Figure 4 were fit to eq 2–4 by the PROPHET nonlinear least-squares fitting routine, using the following protocol. First, the data of Figure 4A were fit to eq 2 to obtain k_{12}, k_{21}, and K_{12} by calculation. The estimate of K_{12} was used with eq 3 to fit the data of Figure 4B to obtain k_{23}, k_{32}, and

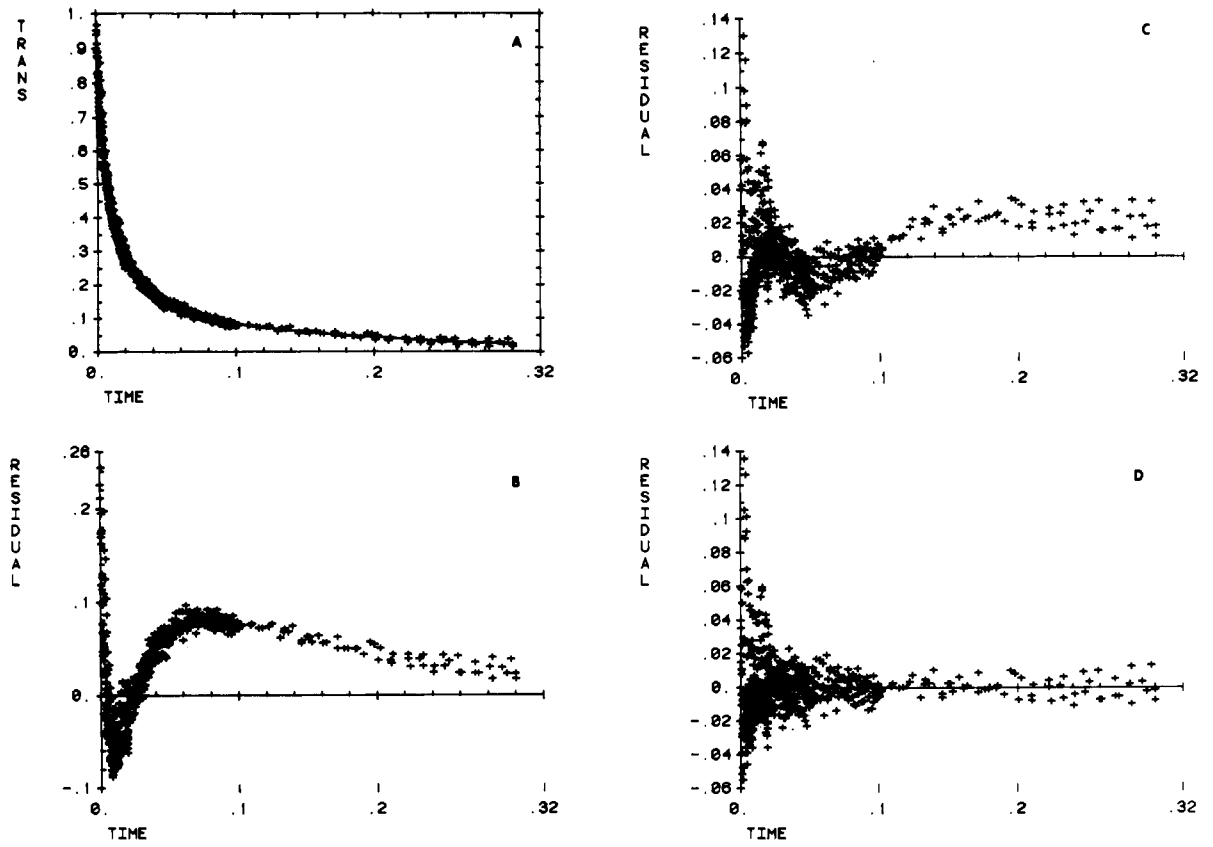

FIGURE 3: Sample composite time course of the association of daunomycin with calf thymus DNA. The change in transmittance at 480 nm (relative to an infinite-time base line) with time is shown. Solution conditions and final concentrations are described in Figure 2. (A) The composite time course was obtained by digitizing and combining 12 photographic traces obtained over a range of time scans, as described in the text. The number of points comprising the composite curve is 511. The data were fit to one-, two-, and three-exponential terms, with the results shown in Table I. The three-exponential fit is indicated by the solid line. Also shown are the residual plots for the (B) one-exponential, (C) two-exponential, and (D) three-exponential fits.

K_{23}. The estimates for K_{12} and K_{23} were used with eq 4 to obtain k_{34} and k_{43} from the data of Figure 4C. The solid lines in Figure 4 indicate the least-squares fits, and the rate constants obtained are summarized in the first row of Table II.

The overall equilibrium constant for Scheme I is given by

$$K_{eq} = K_{12}(1 + K_{23} + K_{23}K_{34})$$

From the kinetic data of Table II, we calculate an overall equilibrium constant of 7.6×10^5 M^{-1} (21 °C), a value in excellent agreement with the binding constant of 7.0×10^5 M^{-1} (20 °C) measured in Figure 1 by the spectrophotometric titration. The excellent agreement of these values lends considerable confidence to our estimates of the rate constants and to the validity of Scheme I as a plausible reaction mechanism.

Temperature-Jump Relaxation Experiments. Temperature-jump experiments in which changes in the absorbance of daunomycin at 480 nm were monitored following a jump from 25 to 33 °C revealed two well-resolved relaxation times of about 2 and 25 ms, corresponding to the fast and intermediate relaxation times, respectively, seen in stopped-flow experiments. The slowest relaxation time seen in the stopped-flow experiments (about 200 ms) might be obscured by the cooling of the T-jump apparatus, and therefore invisible, or the amplitude might be zero in a thermally induced process. The fast temperature-jump relaxation, identified with the bimolecular binding step, was linearly dependent on concentration as shown in Figure 4A. Fit of the experimental data to eq 2 provides estimates for k_{12} and k_{21} at 33 °C, as shown in the bottom row of Table II. Data for the second relaxation observed in T-jump experiments were obtained only over a narrow concentration range [$f(r)C_0 - f'(r)C_f$ = 20–40 μM] and were essentially constant with $1/\tau = 37.4 \pm 4.4$ s.

Table III: Summary of Daunomycin Dissociation Rates As Determined by the SDS Method[a]

T (°C)	k_{32} (s^{-1})	k_{43} (s^{-1})
21.0	5.5 ± 1.2	1.25 ± 0.25
26.0	9.0 ± 1.3	2.0 ± 0.2
33.0	27.0 ± 9.0	7.7 ± 0.5
48.5	43.2 ± 8.0	12.5 ± 3.5

[a] Solution conditions were BPES buffer.

These observations confirm the existence of two of the three relaxations seen in stopped-flow experiments and provide estimates for two of the six rate constants describing Scheme I.

Conventional Stopped-Flow Studies. Two additional stopped-flow studies provide independent estimates of three of the six rate constants for Scheme I. First, the SDS dissociation procedure of Mueller & Crothers (1968), in which drug is dissociated from a preformed drug–DNA complex by mixing with SDS, provides access to dissociation steps.

Figure 5A shows the results of such a dissociation experiment. Two exponentials are required to fit the dissociation curve, as judged by the residual plots of Figure 5B,C and by the improvement of the statistics of the fit. We identify the slower rate with k_{43} and the faster rate with k_{32}. Results over a range of temperatures are shown in Table III. Both of the rates observed by this method were independent of the initial binding ratio, over the range r_b = 0.05–0.2. Identical results were obtained for final SDS concentrations of 0.5% (w/v) or

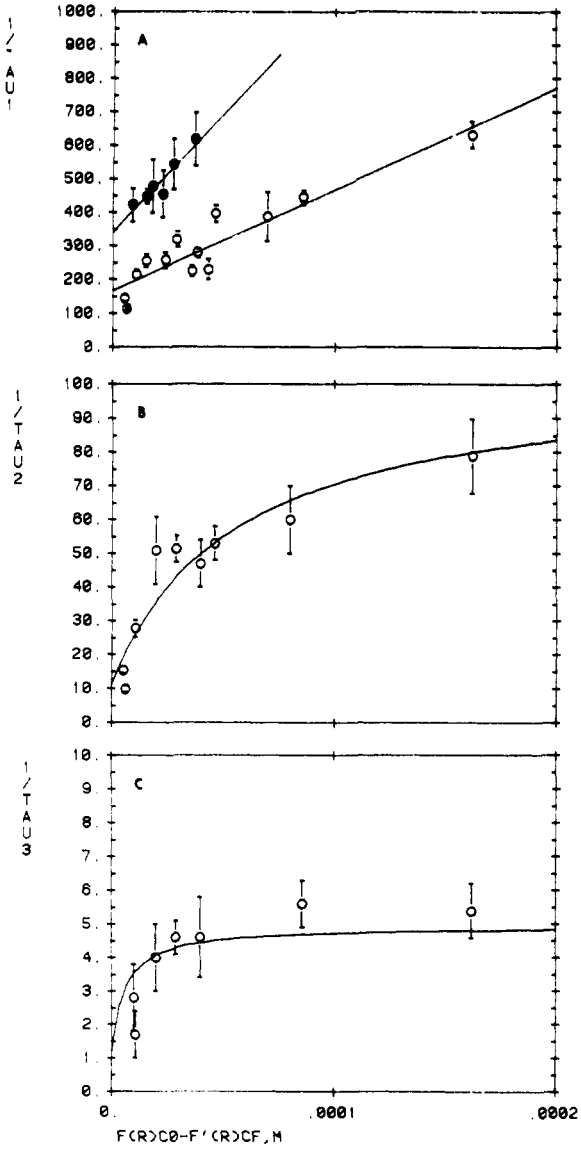

FIGURE 4: Reciprocal relaxation times as a function of concentration. Experimentally determined relaxation times obtained from composite time course curves are shown as a function of the free concentration of reactants. (A) Fast relaxation obtained from stopped-flow measurements at 21 °C (○) or T jump at 33 °C (●). Data were fit to eq 2 by using a linear least-squares fit. (B) Intermediate relaxation time obtained from stopped-flow measurements at 21 °C. The line is the nonlinear least-squares fit of the data to eq 3. (C) Slowest relaxation time obtained from stopped-flow measurements at 21 °C. The line is the least-squares fit of the data to eq 4.

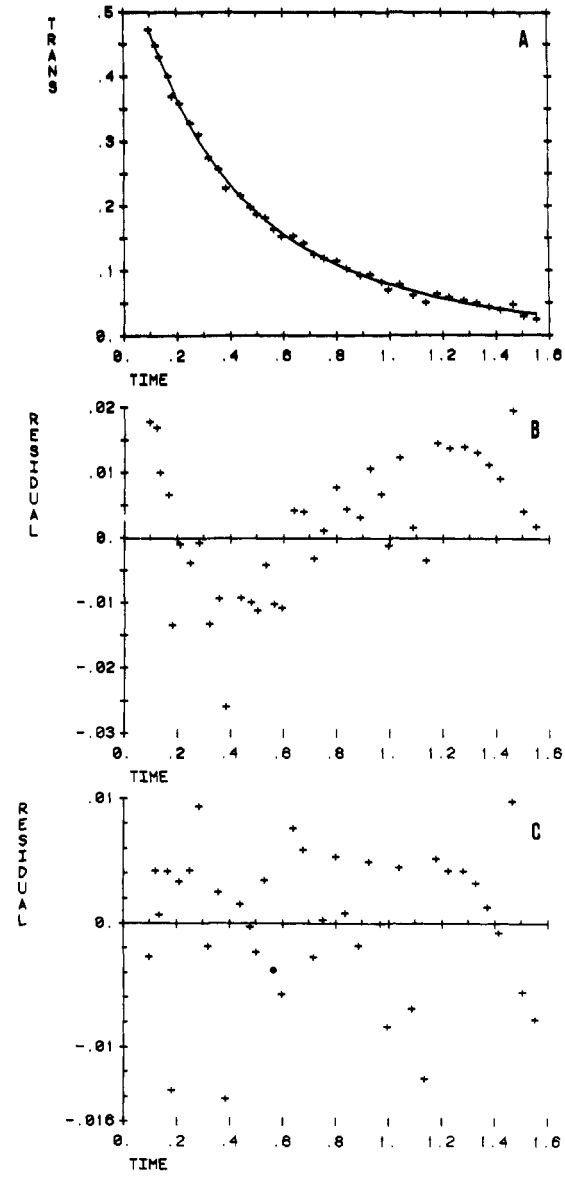

FIGURE 5: Dissociation of daunomycin from DNA. A preformed daunomycin–DNA complex (r_b = 0.05) in BPES were flowed against a 2% SDS solution (in BPES buffer) to affect the dissociation of the drug. Final *total* concentrations were 296 μM (bp) DNA, 15 μM daunomycin, and 1% SDS at 21 °C. Residual plots of fits of the data to one (B) and two (C) exponentials are shown. Changes in transmittance at 480 nm were used to monitor the reaction. Photographs of the oscilloscope traces were digitized as described in the text and fit to singe and multiple exponentials.

1% (w/v). The results from this method are in good agreement with the values for k_{43} and k_{32} estimated from relaxation analysis (Table II), providing independent confirmation of these rate constants.

Figure 6 shows the results of a mixing experiment in which the bimolecular binding step was monitored under pseudo-first-order conditions as a function of total DNA binding site concentration. (The experimental conditions are thus similar to those in the relaxation experiments described above, but the analysis is more conventional.) The apparent first-order rate constant for the fastest step following mixing was obtained by the fitting procedure described above and plotted against the total DNA binding site concentration, as shown in Figure 6. The slope of the line in Figure 6 is k_{12}, and the value of 2.8×10^6 M^{-1} s^{-1} is in excellent agreement with the value of 3.0×10^6 M^{-1} s^{-1} obtained from relaxation analysis of the data of Figure 4.

These additional stopped-flow studies are consistent with Scheme I and provide independent estimates for three of the six rate constants obtained by relaxation analysis, as summarized in Table II.

Activation Energies. The data of Tables II and III allow estimates of the activation energies of some of the steps in Scheme I to be made. The activation energy is defined by the standard relation

$$E^a_{ij} = -R(\mathrm{d} \ln k/\mathrm{d}T^{-1})$$

where E^a_{ij} is the activation energy of going from state i to state j and R is the gas constant. From the rates of 21 and 33 °C for the rapid bimolecular step (Table II), we estimate E^a_{12} = +12.8 kcal/mol and E^a_{21} = +10.7 kcal/mol, corresponding to an enthalpy change for this step of $\Delta H^\circ_{12} = E^a_{12} - E^a_{21}$ = +2.1 kcal/mol. From Table III, we estimate by linear least-squares fitting of the data to the above equation E^a_{32} =

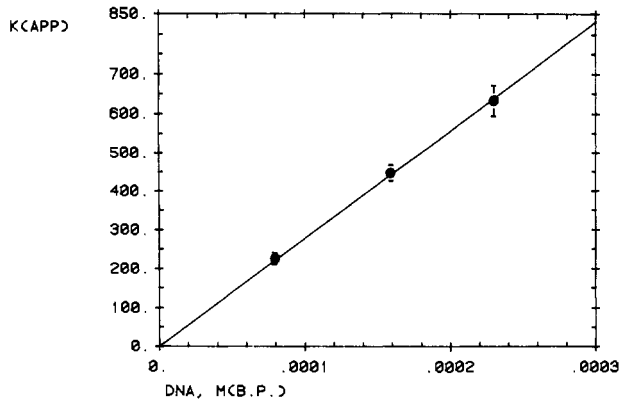

FIGURE 6: Plot of the pseudo-first-order rate constant k(app) vs. DNA concentration. The apparent first-order rate for the binding of daunomycin to DNA was measured as a function of DNA concentration at a constant total daunomycin concentration of 10 μM, in BPES buffer, 21 °C. The slope of the plot is the bimolecular rate constant k_{12} and was found by least-squares analysis to be 2.8×10^6 M^{-1} s^{-1}.

+14.3 kcal/mol and E^a_{43} = +16.2 kcal/mol.

Discussion

The results described here are consistent with a reaction mechanism for the binding of daunomycin to DNA that includes three steps:

$$D + S \rightleftharpoons C_1 \rightleftharpoons C_2 \rightleftharpoons C_3$$

where D represents drug, S potential DNA binding site, and C_i conformers of the drug–DNA complex. The six rate constants for this mechanism as defined by Scheme I and summarized in Table II may be used to calculate an overall equilibrium constant in excellent agreement with that obtained from independent equilibrium measurements.

Interpretation. Our interpretation of this kinetic mechanism in terms of molecular events is as follows. The fast bimolecular step probably represents the formation of a weakly bound, "outside" drug–DNA complex. The small positive enthalpy associated with step 1 (ΔH°_{12} = +2.1 kcal/mol) would be consistent with the formation of a weak ionic complex (Ross & Subramanian, 1981). Further, formation of an intermediate, nonintercalated complex such as proposed seems necessary to hold the drug in the vicinity of DNA to allow time for structural alterations needed for intercalation (e.g., unstacking or opening of base pairs) to occur. The second step in the proposed model would then represent the intercalation of the drug into the DNA helix. The equilibrium constant for this step, K_{23}, is of the same magnitude as reported for similar steps in the binding of proflavin (Li & Crothers, 1969) and tilorone (Sturm, 1982) to calf thymus DNA. The final step in Scheme I may represent a conformational rearrangement of either the intercalated drug molecule or the DNA molecule. Rates of the same magnitude as reported here for this step were reported for some of the isomerizations of the actinomycin–DNA complex (Muller & Crothers, 1968).

Possible Alternate Mechanisms. Scheme I provides the simplest possible mechanism to account for our data and provides excellent quantitative agreement with existing equilibrium data. Scheme I certainly is one valid model for the reaction mechanism. We wish, however, to explore additional models that introduce subtleties. In particular, we first recognize that daunomycin was previously found to show a slight preference for G-C-rich DNA as a binding site (Chaires et al., 1982b) and shows a more dramatic preference toward alternating purine–pyrimidine sequences over nonalternating sequences (Chaires, 1983). How might such sequence specificity manifest itself in our kinetic experiments? Ryan & Crothers (1984) have recently put forth several kinetic models that incorporate transfer steps of bound drug between unique DNA sites. Since we observe clear plateau regions at high concentrations for the slow relaxation times, we omit from discussion models that include bimolecular transfer steps, which are characterized by multiple relaxations that all increase linearly with reactant concentration. Two possible models incorporating sequence specificity remain. First, the "no transfer" model

Scheme II

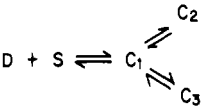

Scheme III

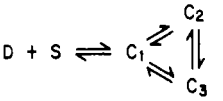

$$S + D \rightleftharpoons C_1$$

$$S + D \rightleftharpoons C_2$$

is one in which the ligand D binds to DNA sites (S) to form two different complexes, C_1 and C_2. The "internal transfer" model

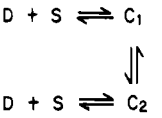

allows for the unimolecular interconversion of the two types of complexes. C_1 and C_2 could represent drug bound at G-C and A-T sites, at alternating purine–pyrimidine or nonalternating sequences, or at the major or minor groove, for example. Both of these mechanisms predict two relaxation times, one of which plateaus at high concentrations. If we extend these models to include a nonintercalated intermediate, two mechanisms result as seen in Schemes II and III. Both of these predict three relaxation times. Assuming the rapid equilibration of the first step and that the rate of the $C_1 \rightleftharpoons C_2$ conversion is greater than that of the $C_1 \rightleftharpoons C_3$ conversion, these models predict two slow relaxations that plateau at high concentrations, in qualitative agreement with what we observe in Figure 4. These schemes thus remain viable, albeit more complex, alternate mechanisms to the sequential model we have selected. To distinguish between these models and the sequential model, the kinetics of drug binding as a function of base composition and sequence need to be studied. Such studies are under way, but the data currently available are insufficient to decide if consideration of the more complex Schemes II and III is warranted. Scheme I remains sufficient to explain our current kinetic observations, satisfies the data on hand, and certainly represents one possible reaction mechanism.

One additional complexity requires discussion. Graves & Krugh (1983) found daunomycin binding to calf thymus DNA to be cooperative and found that their data could be fit by either of two models, a "two-site" model that includes a cooperativity parameter for each site or the allosteric model of Dattagupta et al. (1980). In the latter model, drug binding is coupled to a conformational change in the DNA binding site. A mechanism incorporating this behavior would be

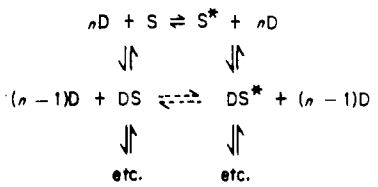

in which D is free drug, S and S* are DNA conformers, and DS and DS* are drug–DNA complexes. This mechanism is analogous to that proposed for the binding of substrate to allosteric enzymes (Eigen, 1968). The model predicts a slow reciprocal relaxation associated with the conformational transition of the DNA that (i) decreases with increasing ligand concentration and (ii) is constant with increasing site concentration. We do not observe such behavior. We note that if we allow intraconversion of the complexes (dashed arrows), pathways identical with our sequential model are available. Thus, while our data neither prove nor disprove cooperative binding, they suggest that if cooperativity does exist, the conformational change in the nucleic acid is not rate limiting and that the preferred binding path follows a sequential scheme more analogous to the "induced-fit" model proposed for allosteric enzymes. We note in connection with this general topic that Sturm (1982) has observed a relaxation step in the binding of tilorone to poly(dA)·poly(dT) that is invariant with ligand concentration which has been assigned to a rate-limiting conformational change in the polynucleotide.

Thermodynamics. We previously have found that daunomycin binding to DNA is characterized by negative enthalpy (Chaires et al., 1982b; Chaires, 1984). Hydrogen bond formation at the intercalation site and coupled conformational changes in the DNA were proposed as the most likely source of this negative enthalpy. Since we find here a small, positive enthalpy for the first step ($\Delta H°_{12}$ = +2.1 kcal/mol), the subsequent steps must be characterized by negative enthalpies. This would be consistent with our interpretation that the actual intercalation event follows the first bimolecular interaction.

Comparison with Previous Work. Kinetic studies on the interaction of daunomycin with DNA are sparse, and we have little to compare our data with. Gabbay et al. (1976) have, using the SDS dissociation method, reported a first-order rate constant of 0.68 s^{-1} for the dissociation of daunomycin from salmon sperm DNA, at 100 mM NaCl, 15 °C. We identify this with our rate constant k_{43}, which we estimate by extrapolation to be 0.78 s^{-1} at 15 °C, in substantial agreement with that obtained by Gabbay et al. Recent ^{31}P NMR measurements indicate an exchange rate of about 1 s^{-1} for the interaction of daunomycin with calf thymus DNA at 20 °C (Jones et al., 1984), a rate in agreement with our estimate for k_{43}. Stutter & Forster (1979) report a single relaxation time of 0.77 ms using temperature-jump methods. Using a first-order Ising chain model and assuming a single-step binding mechanism to interpret their data, they estimate a dissociation constant of about 15 s^{-1} and an association constant of 9.3 × 10^6 M^{-1} s^{-1} at 30 °C. This latter value is in substantial agreement with our estimate of k_{12} at 33 °C (Table II).

A comparison of the kinetics of daunomycin with the mechanism and rates for other DNA binding drugs is of interest. We have for comparison kinetic studies for the intercalators actinomycin (Mueller & Crothers, 1968), ethidium (Bresloff & Crothers, 1975; Ryan & Crothers, 1984), proflavin (Li & Crothers, 1969; Ramestein et al., 1980), and tilorone (Sturm, 1982) and the nonintercalating compounds 2,7-di-*tert*-butylproflavin (Mueller et al., 1973) and irehdiamine A (Dattagupta et al., 1978). A wide variety of reaction mechanisms describe the interaction of these compounds with DNA, ranging from a simple single-step bimolecular reaction mechanism that describes the irehdiamine A–DNA interaction to a complex, six-step branched mechanism required to account for the actinomycin–DNA kinetics. One striking feature to emerge from comparison is that the rates of the isomerization and dissociation steps for the daunomycin–DNA interaction (Table II) are orders of magnitude slower than those reported for the "simple" intercalators ethidium, proflavin, and tilorone, although not as slow as some of the comparable steps reported for the actinomycin–DNA interaction. The interesting and important observation is that the clinically useful compounds actinomycin and daunomycin both have slow isomerization steps along their dissociation pathway, and consequently will be bound to DNA for a longer lifetime relative to the less clinically useful simple intercalators. Very fast dissociation rates, on the order of 10^3 s^{-1}, characterize the nonintercalating 2,7-di-*tert*-butylproflavin and irehdiamine A, in contrast to the intercalating compounds.

Daunomycin shares with other intercalators a bimolecular rate constant of 10^6–10^7 M^{-1} s^{-1}. This is slightly less than what might be anticipated for a diffusion-controlled encounter, as probably represented by the values of about 10^8 M^{-1} s^{-1} found for the nonintercalating compounds.

Finally, the variety of both mechanisms and rates among intercalating compounds is noteworthy. Even though these compounds all intercalate, and produce similar structural alterations in DNA, there is apparently no common mechanism or pathway leading to the final intercalation complex.

Added in Proof

After this work was completed and submitted for publication, an article appeared describing temperature-jump kinetic studies on the interaction of anthracycline antibiotics with calf thymus DNA (Forster & Stutter, 1984). For daunomycin, two relaxation times are reported, which correspond to the two faster relaxation times we observe in our stopped-flow experiments and which agree with our temperature-jump observations.

Registry No. Daunomycin, 20830-81-3.

References

Arcamone, F. (1981) *Doxorubicin: Anticancer Antibiotics*, Academic Press, New York.

Barthelemy-Clavey, V., Molinier, C., Aubel-Sadron, G., & Maral, R. (1976) *Eur. J. Biochem. 69*, 23–33.

Bresloff, J. L., & Crothers, D. M. (1975) *J. Mol. Biol. 95*, 103–123.

Chaires, J. B. (1983a) *Biochemistry 22*, 4204–4211.

Chaires, J. B. (1983b) *Nucleic Acids Res. 11*, 8485–8494.

Chaires, J. B. (1985) *Biopolymers* (in press).

Chaires, J. B., Dattagupta, N., & Crothers, D. M. (1982a) *Biochemistry 21*, 3927–3932.

Chaires, J. B., Dattagupta, N., & Crothers, D. M. (1982b) *Biochemistry 21*, 3933–3940.

Chaires, J. B., Dattagupta, N. D., & Crothers, D. M. (1983) *Biochemistry 22*, 284–292.

Crothers, D. M. (1968) *Biopolymers 6*, 575–584.

Crothers, D. M. (1971) in *Procedures in Nucleic Acids Research* (Davies, D. R., Ed.) Vol. 2, pp 369–388, Harper and Row, New York.

Dattagupta, N., Hogan, M., & Crothers, D. M. (1978) *Proc. Natl. Acad. Sci. U.S.A. 75*, 4286–4290.

Dattagupta, N. D., Hogan, M., & Crothers, D. M. (1980) *Biochemistry 19*, 5998–6005.

DiMarco, A., Zunnio, F., Silverstrini, R., Gambarucci, C., & Gambetta, R. A. (1971) *Biochem. Pharmacol. 20*, 1323–1328.
Eigen, M. (1968) *Q. Rev. Biophys. 1*, 3–33.
Forster, W., & Stutter, E. (1984) *Int. J. Biol. Macromol. 6*, 114–124.
Fritzche, H., Triebel, H., Chaires, J. B., Dattagupta, N., & Crothers, D. M. (1982) *Biochemistry 21*, 3940–3946.
Gabbay, E. J., Grier, D., Fingerle, R. E., Reimer, R., Levy, R., Pearce, S. W., & Wilson, W. D. (1976) *Biochemistry 15*, 2060–2070.
Gianni, L., Corden, B. C., & Meyer, C. E. (1982) *Rev. Biochem. Toxicol. 5*, 1–82.
Goodman, M. F., Lee, G. M., & Bachur, N. R. (1977) *J. Biol. Chem. 252*, 2670–2674.
Graves, D. E., & Krugh, T. R. (1983) *Biochemistry 22*, 3941–3947.
Hartmann, G., Goller, H., Koschel, K., Kersten, W., & Kersten, H. (1964) *Biochem. Z. 341*, 126–128.
Hiromi, K. (1979) in *Kinetics of Fast Enzyme Reactions*, pp 218–219, Halsted Press, New York.
Jones, R. L., Yen, S.-F., & Wilson, W. D. (1984) *Biophys. J. 45*, 114a.
Jovin, T. M., & Stricker, G. (1977) in *Chemical Relaxation in Molecular Biology* (Pecht, I., & Rigler, R., Eds.) pp 245–282, Springer-Verlag, New York.
Li, H. J., & Crothers, D. M. (1969) *J. Mol. Biol. 39*, 461–477.
McGhee, J. D., & von Hippel, P. H. (1974) *J. Mol. Biol. 86*, 469–489.
Mirau, P. A., & Kearns, D. R. (1983) *Nucleic Acids Res. 11*, 1931–1941.
Mueller, W., & Crothers, D. M. (1968) *J. Mol. Biol. 35*, 251–290.
Mueller, W., Crothers, D. M., & Waring, M. (1973) *Eur. J. Biochem. 34*, 223–234.
Ramestein, J., Ehrenbers, M., & Rigler, R. (1980) *Biochemistry 19*, 3938–3948.
Ross, P. D., & Subramanian, S. (1981) *Biochemistry 20*, 3096–3102.
Ryan, D. P., & Crothers, D. M. (1984) *Biopolymers 23*, 537–562.
Scatchard, G. (1949) *Ann. N.Y. Acad. Sci. 51*, 660–672.
Schellinx, J. A. A., Dijkwel, P. A., & Wanka, F. (1979) *Eur. J. Biochem. 102*, 409–416.
Sturm, J. (1982) *Biopolymers 21*, 1189–1206.
Stutter, E., & Forster, W. (1979) *Stud. Biophys. 75*, 199–208.
Ward, D. C., Reich, E., & Goldberg, I. H. (1965) *Science (Washington, D.C.) 149*, 1259–1263.

Donor Activation in the T_4 RNA Ligase Reaction

Larry W. McLaughlin,* Norbert Piel, and Erika Graeser

Max-Planck-Institut für experimentelle Medizin, Abteilung Chemie, D-3400 Göttingen, Federal Republic of Germany
Received December 27, 1983; Revised Manuscript Received August 28, 1984

ABSTRACT: T_4 RNA ligase catalyzes the adenylation of donor oligonucleotide substrates. These activated intermediates react with an acceptor oligonucleotide which results in phosphodiester bond formation and the concomitant release of AMP. Adenylation of the four common nucleoside 3′,5′-bisphosphates as catalyzed by T_4 RNA ligase in the absence of an acceptor oligonucleotide has been examined. The extents of product formation indicate that pCp is the best substrate in the reaction and pGp is the poorest. Kinetic parameters for the joining reaction between the preadenylated nucleoside 3′,5′-bisphosphates, A(5′)pp(5′)Cp or A(5′)pp(5′)Gp, and a good acceptor substrate (ApApA) or a poor acceptor substrate (UpUpU) have been determined. The apparent K_m values for both preadenylated donors in the joining reaction are similar, and the reaction velocity is much faster than observed in the overall joining reaction. The nonnucleotide adenylated substrate P^1-(5′-adenosyl) P^2-(*o*-nitrobenzyl) diphosphate also exhibits a similar apparent K_m but reacts with a velocity 80-fold slower than the adenylated nucleoside 3′,5′-bisphosphates. By use of preadenylated donors, oligonucleotide substrates can be elongated more efficiently than occurs with the nucleoside 3′,5′-bisphosphates.

While T_4 RNA ligase is useful in catalyzing the formation of a phosphodiester bond between an acceptor oligonucleotide and a corresponding donor (Gumport & Uhlenbeck, 1981; Uhlenbeck & Gumport, 1982) and can be used with some success with similar 2′-deoxyoligonucleotides (Hinton et al., 1978; Hinton & Gumport, 1979; McCoy & Gumport, 1980), its effectiveness is limited in that it does not work equally well with all oligonucleotide sequences (England & Uhlenbeck, 1978; Romaniuk et al., 1982). Generally acceptors with a high purine content and pyrimidine-containing donors result in the highest yields of joined product. However, acceptor molecules of the same nucleoside composition but differing sequence can nevertheless react with a common donor and result in vastly different product yields (Romaniuk et al., 1982).

The mechanism of phosphodiester bond formation as catalyzed by the enzyme is similar to that which has been elucidated for DNA ligase (Modrich & Lehman, 1973; Lehman, 1974) although the substrate specificities are different. DNA ligase requires a double-stranded substrate and RNA ligase is more active with single-stranded substrate. Three distinct and reversible steps are involved (Uhlenbeck & Cameron, 1977; Sugino et al., 1977). In the first step the enzyme reacts with ATP to form an adenylated enzyme intermediate and pyrophosphate. In the second step the enzyme binds a donor molecule containing a 5′-terminal phosphate and catalyzes the formation of the adenylated donor: A(5′)pp(5′)Np.... Subsequently, the formation of a phosphodiester bond occurs between the acceptor and activated donor with concomitant

0006-2960/85/0424-0267$01.50/0